

## **ANALYSIS OF INTENSIFIED REVERSE DEEP DRAWING PROCESS**

**Toshko Marinov KOVACHEV\***

### **ABSTRACT**

This article presents an analysis of intensified process for manufacturing rotational parts from thin sheet material by means of reverse hydro-mechanical deep drawing. A comparison has been made between reverse hydro-mechanical deep drawing and available conventional technology of manufacturing thin-walled parts. Intensification of deformation route, peculiar to these processes, is estimated through deformation charts; boundary shape strain charts and the stressed state index  $\Pi_{\infty}$ . Correlative statistical relationships are also provided by means of which the values of  $\varepsilon_r$ ,  $\varepsilon_{\theta}$  and  $\varepsilon_z$  are calculated where by it is possible to draw related deformation charts.

*Keywords: Deep Drawing, Intensification, Shaping*

## **YOĞUNLAŞTIRILMIŞ TERS DERİN ÇEKME İŞLEMİNİN ANALİZİ**

### **ÖZET**

Sunulan makale, ters hidro-mekanik derin çekme yöntemiyle ince sac malzemeden dönel simetrik parçaların üretiminde yoğunlaştırılmış işlemin analizini vermektedir. Çalışmada ayrıca, ters hidro-mekanik derin çekme ile ince cidarlı parçaların üretimindeki klasik derin çekme teknolojileri karşılaştırılmıştır. Belirtilen işlemlere özgü şekil değiştirme yörüngesinin yoğunlaştırılması şekil değiştirme diyagramları, sınır genleme diyagramları ve  $\Pi_{\infty}$  gerilme hali endeksi yardımıyla hesaplanmıştır. Çalışmada  $\varepsilon_r$ ,  $\varepsilon_{\theta}$  ve  $\varepsilon_z$  değerlerinin hesaplanmasını da sağlayan istatistik yaklaşımlar da sunulmuştur.

*Anahtar Kelimeler: Derin Çekme, Yoğunlaştırma, Şekil Verme*

---

\*Department "MTM" of Technical University – Gabrovo

## **1. INTRODUCTION**

Recent development of technologies underlying mechanical shaping aims at manufacturing of complete products; the main target being the intensification of deformation route and production of defect free parts. This in turn requires a comprehensive estimate of both stressed and strained states of the materials used and their manufacturing ductility with regard to most efficient use of their ductile properties.

Employment of conventional methods of machining by means of plastic deformation will be encumbered because of the inadequate manufacturing ductility of the materials in use as well as the development of negative friction processes between material and tool, the tendency to cause local defects and destruction (Tomlenov 1972; Evstratov 1981). There are a number of means used to overcome mentioned problems, but with fairly low effect such as coatings, lubricants, varnishes, chemical treatment in solutions, longer deformation route, special heat treatment between different operational stages, cleansings etc. which, in the end, make the product very costly.

Recently, there has been a marked tendency for shaping to be effected in either elastic or liquid medium or in combination with inflexible punches. Investigations have indicated (Kostov and Kovachev 1994; Kostov 1992; Kostov 1994; Kostov 1996) good prospects for reverse hydro-mechanical deep drawing (RHDD).

The basic aim of this article is to make comparative analyses of both intensified reverse deep drawing process and conventional multiple transition manufacturing process.

## **2. SIMPLIFIED DIAGRAMS OF CONVENTIONAL DEEP DRAWING (CDD) AND REVERSE HYDRO-MECHANICAL DEEP DRAWING (RHDD)**

### **2.1. Conventional Deep Drawing**

Conventional deep drawing can be achieved without a blank holder as indicated in Figure 1, or with a blank holder as shown in Figure 2 (Malinin 1975; Popov 1977). Normally, the first method employs conventional drawing punches which consist of a matrix 1 and punch 2. It is used for manufacturing shallow vessels or thin walled articles with no folds or corrugation. Figure 1-b presents the second stage of deep drawing without a blank holder.

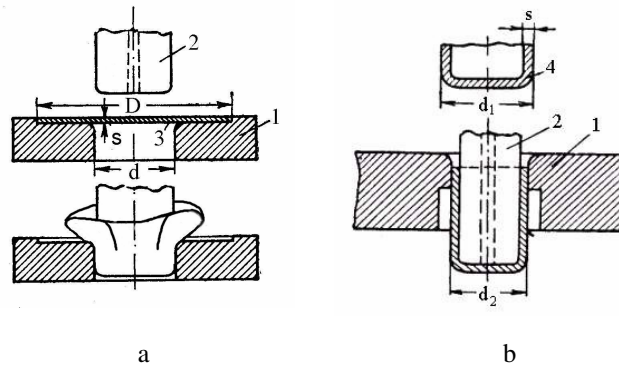


Figure 1 Conventional deep drawing without blank holder

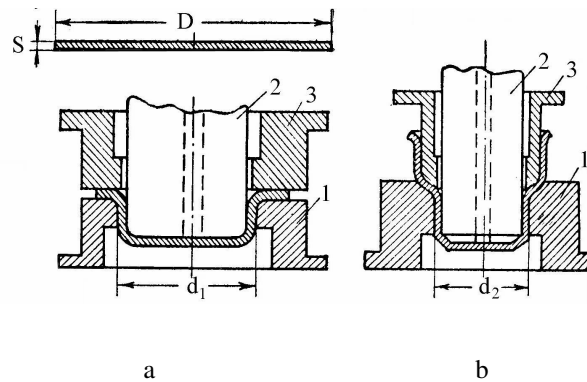


Figure 2 Conventional deep drawing with blank holder

Blank holder 3 is used in the second method of deep drawing shown on Figure 2. The collar section of the work piece is pressed against the matrix by blank holder in order to prevent corrugation forming on the material, as the material is forced downwards through matrix hole under the punch pressure. Figure 2-a shows the first stage of deep drawing by punching a flat work piece whereas Figure 2-b shows the second stage of drawing the hollow work piece.

## 2.2. Reverse Hydro-mechanical Deep Drawing (RHDD)

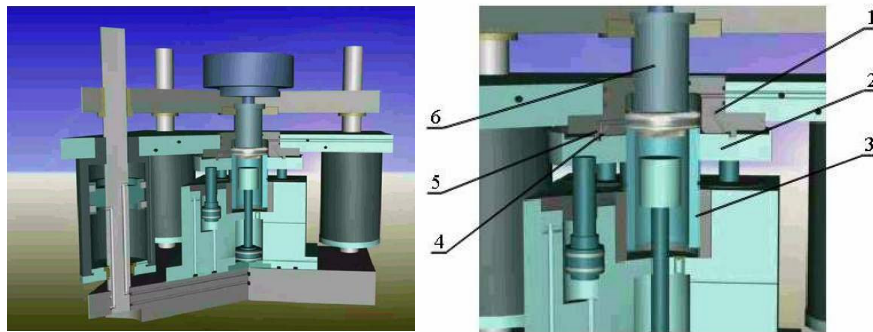


Figure 3 Schematic illustration of drawing punches for RHDD

The process of shaping is characterized by reversing the work piece and keeping the material under hydraulic compression in all round that alters the frictional conditions ( Figure 3 and 4 ). Three-dimensional shaping of the blanks is a continuous process (Figure 4) which is characterized by employing several peculiar stages.

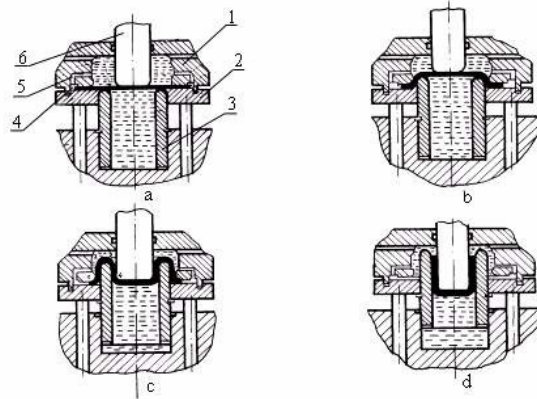


Figure 4. Schematic illustration of RHDD stages

Drawing die 1 in Figure 3, whose chamber is filled with oil beforehand, overcomes the opposing compression of the hydraulic clamp 2 and initiates drawing of the blank part over the punch 3. Due to the progressively growing pressure within the chamber 1 oil starts flowing along the channels 5 and then into channel 4 thus exerting radial pressure along the periphery of the blank part. Upon consequent downward stroke of puncheon 6, the blank part is inserted into its receptive aperture 3. This causes oil pressure to increase thus exerting pressure against the lower base of the punch 3 which is pushed upward and impacts this section of the blank that is inserted between the puncheon 6 and mould 1. The opposing motion of the punch 3, the mould 1 and the clamp 2 which is in permanent contact in relation to the puncheon 6 is adjusted and synchronized electro-hydraulically. General view of the test unit with its attachments and instrumentation is shown on Figure 5.

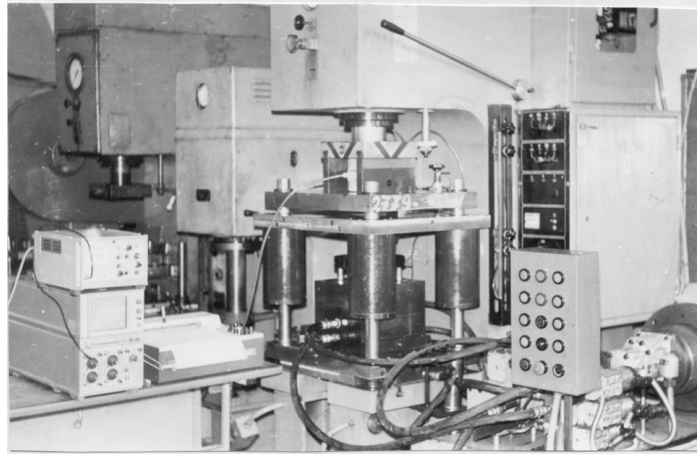


Figure 5 General view of the test unit for RHDD

### **3. LEVEL OF INTENSIFICATION ESTIMATE**

The level of intensity of manufacturing rotational pieces from thin sheet material by means of reverse hydro-mechanical deep drawing is estimated through the innate engineering ductility and the index of stressed state.

Engineering ductility is estimated through its entire capacity which includes the amount of expended ductility and the amount of remnant ductility. It is also estimated through deformation charts and the charts presenting boundary forming. This estimate is used in the article to examine, compare and analyze the ductility in multiple conventional deep drawing (CDD) and reverse hydro-mechanical deep drawing in which the work piece is being formed in all-round hydraulic pressure conditions.

Special objects of the presented study are thin sheet rotational parts made of sheet steel 08 KII (Bulgarian State Standard 4959-82) having thickness of  $t = 1,0$  mm with  $C = (0,05 \div 0,11)\%$ ,  $Si = 0,03\%$ ,  $Mn = (0,25 \div 0,5)\%$ , coefficient of normal anisotropy of  $R = 1,16$  and strain hardening coefficient of  $n = 0,19$ . Parameters of products such as a having diameter  $d = 68,0$  mm and height of  $h = 71,0$  mm are used as examples of conventional three stage process of CDD with coefficients of drawing of  $m_1=0,61$ ;  $m_2=0,83$ ;  $m_3=0,85$ .

These processes are investigated by map graticule method, whereby the change of grid elements is used to estimate the value of radial  $\epsilon_r$ , tangential  $\epsilon_\theta$  and normal  $\epsilon_z$  deformation along the generating line of drawn pieces.

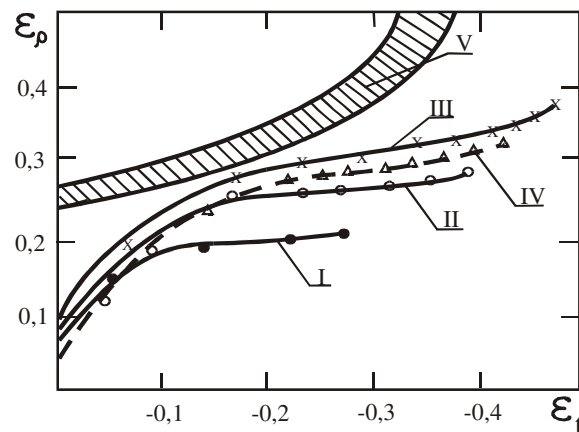


Figure 6 Deformation charts of first (I), second (II) and third (III) phases of conventional deep drawing and reverse hydro-mechanical deep drawing – IVth phase plus diagrams of boundary forming-V

The values of these deformations are mapped in three dimensional map graticule  $\epsilon_r - \epsilon_\theta - \epsilon_z$  according to relevant deformation levels starting from their relative height of drawing as well as in two dimensional map graticule:  $\epsilon_r - \epsilon_\theta$ . Thus we obtain the chart of deformations as presented in Figure 6 and the generalized deformations chart presented in Figure 7.

Deformation charts can be drawn by the values for  $\epsilon_r$  and  $\epsilon_\theta$  which are calculated in accordance with the correlative statistic relationships. The mentioned relationships are obtained through the data concerning investigation of stressed and deformed state and processed by HP9845B. Here are used standard subroutines/programs for analytical interpretation of various relationships. Correction of output data and the proper selection of approximating polynomial are done by the finite differences method.

$$\epsilon_{r,\theta,z} = A_0 + A_1 \cdot \left(\frac{h}{d}\right) + A_2 \cdot \left(\frac{h}{d}\right)^2 + A_3 \cdot \left(\frac{h}{d}\right)^3 + \dots + A_n \cdot \left(\frac{h}{d}\right)^n \quad (1)$$

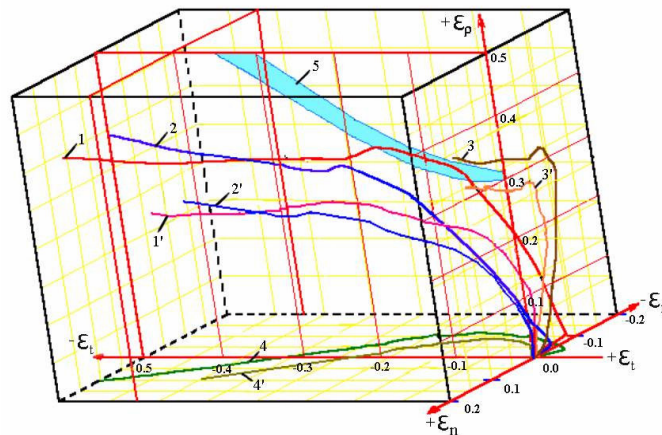


Figure 7. Generalized deformation charts in conventional deep drawing :  
 1 represents  $\epsilon_r - \epsilon_\theta - \epsilon_z$ ; 2 represents  $\epsilon_r - \epsilon_\theta$ ; 3 represents  $\epsilon_r - \epsilon_z$ ; 4 represents  $\epsilon_\theta - \epsilon_z$  and reverse hydro-mechanical deep drawing 1'  $\epsilon_r - \epsilon_\theta - \epsilon_z$ ; 2'  $\epsilon_r - \epsilon_\theta$ ; 3'  $\epsilon_r - \epsilon_z$ ; 4'  $\epsilon_\theta - \epsilon_z$  and diagrams of boundary forming 5.

The coefficients of  $A_0, A_1, A_2, A_3 \dots A_7$  in equation 1 are obtained and summarized in Table 1. Boundary forming diagrams are laid out according to Keller-Goodwin

method (Keeler 1971) by using destruction deformations and the methods presented in (Kostov 1992).

When drawing charts of boundary forming we can note a kind of dissipation of both radial and tangential deformations. It has resulted from deviations in determining the parameters of coordinate circles. Samples are selected with coordinate locations that come within the area of destruction, whereby their surface of destruction goes through their centre or close to it.

Figure 6 presents the field of ultimate strain where the hatched area contains the boundary values of deformations  $\epsilon_r$  and  $\epsilon_\theta$  for steel type 08KII. Destruction begins when the ratio between these deformations corresponds to the values of the lower boundary of the field.

Ductility margins are determined by the mutual position (Figure 6) between the diagrams of boundary forming (V) and the deformations curves (I, II, III and IV), the remainder ductility margin being estimated by the distance these curves withstand from each other.

Comparing these curves will reveal that the remainder ductility margin in reverse hydro-mechanical deep drawing is larger than the margin at the final phase of conventional deep drawing (see Figure – curve I). This fact is confirmed by Figure 7 as well which contains the disposition of summary deformation charts and the diagrams of boundary forming in reverse hydro-mechanical deep drawing and conventional deep drawing (Stage III) of work pieces made of steel 08 KII.

Intensification of deformation route of drawing is also estimated by the variation of the index of stressed state  $\Pi_{\sigma_0}$ : the latter characterizes the rigidity of intensification scheme and is determined, according to V. L. Kolmogorov (1977), by:

$$\Pi_{\sigma_0} = \frac{\sigma}{T} \quad (2)$$

$$\sigma = \frac{1}{3} (\sigma_r + \sigma_\theta + \sigma_z) \quad (3)$$

where  $\sigma$  is the average normal stress and T stands for the intensity of tangential stresses.

Table 1: Coefficients of  $A_0, A_1, A_2, A_3, \dots$  those are obtained from equation 1.

$$\varepsilon_{r,\theta,z} = A_0 + A_1 \left(\frac{h}{d}\right) + A_2 \left(\frac{h}{d}\right)^2 + A_3 \left(\frac{h}{d}\right)^3 + \dots + A_n \left(\frac{h}{d}\right)^n$$

| No        | $\varepsilon_{r,\theta,z}$ | $\varepsilon_{r,\theta,z} = A_0 + A_1 \left(\frac{h}{d}\right) + A_2 \left(\frac{h}{d}\right)^2 + A_3 \left(\frac{h}{d}\right)^3 + \dots + A_n \left(\frac{h}{d}\right)^n$ |         |          |           |           |          |          |          |
|-----------|----------------------------|--|---------|----------|-----------|-----------|----------|----------|----------|
|           |                            | $A_0$  | $A_1$   | $A_2$    | $A_3$     | $A_4$     | $A_5$    | $A_6$    | $A_7$    |
| Phase I   | $\varepsilon_r$            | 0,0244   | 1,3740  | -2,400   |           |           |          |          |          |
|           | $\varepsilon_\theta$       | 0,0089   | -0,9134 | 0,4286   |           |           |          |          |          |
|           | $\varepsilon_z$            | -0,0199  | -1,4238 | 8,7428   | -11,3333  |           |          |          |          |
| Phase II  | $\varepsilon_r$            | 0,0184   | 2,5289  | -9,1902  | 14,2475   | -7,8788   |          |          |          |
|           | $\varepsilon_\theta$       | 0,0194   | -1,2432 | 2,1291   | -2,8314   | 1,6382    |          |          |          |
|           | $\varepsilon_z$            | -0,0368  | -2,3538 | 24,2762  | -109,4704 | 260,337   | -306,343 | 139,574  |          |
| Phase III | $\varepsilon_r$            | 0,0267   | 2,2064  | -5,9723  | 6,8073    | -2,7156   |          |          |          |
|           | $\varepsilon_\theta$       | 0,0247   | -1,0654 | 0,4615   | 0,6618    | -0,5681   |          |          |          |
|           | $\varepsilon_z$            | -0,047   | -1,6078 | 10,0882  | -23,6352  | -29,2597  | -19,3688 | 5,4413   |          |
| RHDD      | $\varepsilon_r$            | 0,0044   | 1,3892  | 1,9637   | -28,0147  | 77,5083   | -98,9995 | 61,528   | -15,0607 |
|           | $\varepsilon_\theta$       | 0,0046   | 0,1907  | -12,5247 | 60,0606   | -135,0132 | 160,146  | -96,7767 | 23,4994  |
|           | $\varepsilon_z$            | -0,0090  | -1,5799 | 10,561   | -32,0459  | 57,5042   | -61,1458 | 35,2473  | -8,4388  |

$$T = \frac{1}{\sqrt{6}} \sqrt{(\sigma_r - \sigma_\theta)^2 + (\sigma_\theta - \sigma_z)^2 + (\sigma_z - \sigma_r)^2} \quad (4)$$

Figure 8 presents the change in the  $\Pi\sigma_0$  index depending on relative height  $h/d$  and Figure 9 presents that change according to height ( $h$ ) of work pieces made of steel type 08KП. These index increments are changed from the upper peripheral end of the piece towards the critical section and the bottom center. In the three stage process of drawing, the index  $\Pi\sigma_0$  is changed in the area of the critical section within the following limits  $\Pi^I\sigma_0 = +0.635$ ,  $\Pi^{II}\sigma_0 = +0.681$  and  $\Pi^{III}\sigma_0 = +0.717$ .

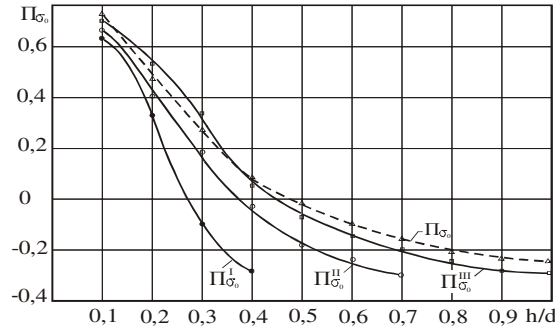


Figure 8 Change in the stressed state index  $\Pi\sigma_0$  depending on relative height  $h/d$

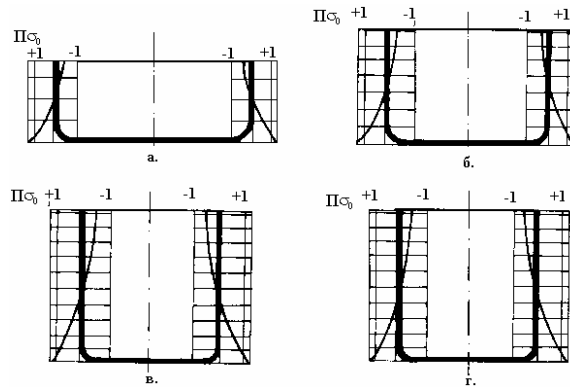


Figure 9 Change in the stressed state index  $\Pi\sigma_0$  according to height ( $h$ ) of work pieces

Almost identical rigidity in the stressed state  $\Pi\sigma_0 = +0,722$  in the area of critical section is characteristic for the intensified reverse process. Drawing upon the phenomenological theory of destruction developed by V.L.Kolmogorov (1977) and ductility performance diagram for steel type 08KII, in particular, we can note that with intensified deformation process nearly the same boundary level of deformation is retained in the area of critical section whereas in all other sections it is higher as compared to conventional drawing.

#### **4. CONCLUSIONS**

The level of intensification of manufacturing rotational pieces from thin sheet material by reverse hydro-mechanical deep drawing is estimated by means of deformation charts, boundary forming diagrams and the stressed state index. Distribution of stresses and the relevant index  $\Pi\sigma_0$  determine instances of stressed state where the rigidity of each constituent element of the piece is lower than or, at least, equal to those in conventional drawing.

#### **REFERENCES**

- Evstratov, V.A., (1981), Metal Machining Theory, Higher Institute, Harkov.
- Keeler,S.P., (1971), Sheet Metal Industries, No. 9, 36-42.
- Kolmogorov,V.L. and Bogatav A., (1977), Ductility and Destruction, Metallurgy , Moscow.
- Kostov E.S., (1992), About Ductility Margin in Deep Drawing with Intensified Deformation Route, Mechanical Engineering Journal No.12.
- Kostov E.S. and Kovachev T.M., (1994), Reverse Hydromechanic Drawing, Forging and Punching, No. 7, 27-31.
- Kostov E.S., (1994), Improving the Processes and Machinery for Intensified Deep Drawing of Pieces Made of Thin Sheet Material, Anniversary Collection of Articles of Technical University, Gabrovo, 11 – 19.
- Kostov E.S., (1996), On the Parameters of Stressed State during Deep Drawing, Reflections on Technology Journal No. 2, 53-60.
- Malinin,N.N., (1975), Application Theory of Ductility, Mechanical Engineering, Moscow.
- Popov, E.A., (1977), Basic Principles of Sheet Punching Theory, Mechanical Engineering, Moscow.
- Tomlenov,A.D., (1972), Theory of Metal Plastic Deformation, Metallurgy, Moscow.